PHYSICAL REVIEW D VOLUME 8, NUMBER 1 1 JULY 1973

Slope of Diffraction Scattering and Effective Shape of Spectral Functions

B. B. Deo and M. K. Parida
Physics Department, Utkal University, Bhubaneswar-4, Orissa, India
(Received 4 October 1972)

Using considerations of Mandelstam analyticity and conformal mapping, we have related the slope parameters for the forward peaks of pp, $\bar{p}p$, K^+p, and K^-p elastic scattering to equations for the boundaries of spectral functions. From an analysis of the existing data for large values of energies, the effective shape of different spectral functions has been computed.

I. INTRODUCTION

Simple Regge theory has not been very successful in explaining the recent high-energy data on hadron-hadron scattering.[1] It is felt that at least for exotic channels, background scattering could be more adequately treated by methods other than Regge, Pomeranchukon, and cut-exchange theories. In a dynamical theory of strong interactions the observed scattering of particles and hadrons is due to forces generated by exchange of quanta. This is reflected in the analytic structure of the scattering amplitude. During the early stages of development of the dynamics of strong interactions it was recognized that a scattering amplitude constructed to satisfy crossing, analyticity, and unitarity would satisfactorily explain the scattering phenomenon. However, with the discovery of innumerable resonances this program was not found feasible and Regge theory was used extensively. With the high-energy data now available beyond the resonance region, certain general features of the scattering processes have become obvious. The present work is aimed at an attempt to confirm certain analytic properties of the scattering cross sections from the over-all grossly smooth behavior of these observations over a large energy range. Specifically we shall try to relate the start of the singularity in the scattering amplitude to the observed changes in cross sections.

Elastic scattering near forward angles can be fitted by a simple exponential of the type

$$\frac{d\sigma}{dt}=\left(\frac{d\sigma}{dt}\right)_{t=0}e^{b(s)t} \qquad (1)$$

over a large energy range. The forward non-Coulombic peak is quite pronounced and Regge theory predicts that $b(s)\sim\ln s$, which is fairly well verified in intermediate- to high-energy range for a large number of strong-interaction particle scattering processes. One can therefore hypothesize that near the forward angles, the scattering amplitude is almost pure imaginary. Furthermore, in one-pion-exchange processes the contribution from the real part due to the one-pion term vanishes in the forward direction. Therefore the existence of the pseudoscalar pole will not cause much trouble in the analysis near the forward direction. The cut structure of the imaginary part of the amplitude is determined by the region where the double spectral function is nonvanishing. For example, in pp scattering, the spectral function ρ_{st} has a boundary defined by

$$\begin{aligned} t&=t_{\text{in}}(s)\\ &=4m_\pi^2+\frac{4m_\pi^4}{s-4m^2}\,. \end{aligned} \qquad (2)$$

For a given s, a right-hand cut would start from $t_{\text{in}}(s)$.

In a similar context of studying the analytic structure of scattering amplitude, the pole singularity in the amplitude was first demonstrated by Taylor, Moravcsik, and Uretsky,[2] who used the Chew-Low[3] extrapolation in the analysis of experimental data. Improvements have been worked out by Cutkosky and Deo.[4] To obtain the fastest rate of convergence of a series, Cutkosky and Deo[5] and Ciulli[6] have suggested the use of conformally mapping the entire plane of analyticity into the figure of convergence. It has now been demonstrated[5,7,8] that the rate of decrease of the successive coefficients is related to the distance of the physical region from the nearest cut, a farther away cut implying a faster decrease. Using these ideas we shall fit the experimental data to the exponential of a conformally mapped variable z,

$$\begin{aligned} z&\equiv z(s,t)\\ &\equiv z(t_{\text{in}}(s),t)\,. \end{aligned} \qquad (3)$$

From the best fit, one can obtain $t_{\text{in}}(s)$ which can be easily related to $b(s)$, as will be discussed later.

The plan of the paper is as follows. In Sec. II we review the experimental results for slope parameters for pp, $\bar{p}p$, K^+p, and K^-p elastic scattering and discuss the predictions of some successful models. In Sec. III we obtain a parabolic variable by suitably mapping the $\cos\theta$ plane. Section IV deals with the theoretical formulas for slope parameters for various processes and how different formulas can be summarized in a single generalized formula. In Sec. V we show how to obtain the effective shape of spectral functions by matching the experimental data with our analytic formula. In Sec. VI we discuss our results.

II. REVIEW OF EXPERIMENTAL DATA AND THEORETICAL MODELS

Experimental data[9-13] on pp scattering show that the slope of the forward elastic differential cross section increases with energy above laboratory momentum 20 GeV/c. Up to 70 GeV/c there is a steady rate of shrinking. New high-energy data[10-13] from Serpukhov and the CERN Intersecting Storage Rings (ISR), however, suggest that shrinking has slowed and that the slope behaves nearly as $\ln(\ln s)$ above 500 GeV/c. It is also observed[11-13] that as $|t|$ decreases the slope parameters for pp elastic scattering near forward angles at fixed energy increase considerably. There has also been observed a significant change in slope parameters near the crossing point $|t| \sim 0.1$ GeV^2. Available experimental data[9] for the slopes of forward diffraction peaks of $\bar{p}p$ elastic scattering are too erratic to draw any definite conclusion and are attributed to the presence of low-energy resonances which causes the slope to oscillate markedly about a mean value. Above laboratory momentum 8 GeV/c one can roughly say that the slope parameter $b_{\bar{p}p}$ has reached its asymptotic limit of about 12.7 GeV^{-2}.

Models have been proposed to explain experimentally observed facts and none of them have been able to explain adequately all the existing data on pp, $\bar{p}p$, K^+p, and K^-p elastic scattering. Regge-pole theory predicts that the slope of the diffraction peak shrinks as $\ln s$. A linear extrapolation in $\ln s$ from the Serpukhov data to the slopes of pp scattering gives a poor fit as seen in our graph (curve III, Fig. 3).

Kaplan and Schiff,[14] taking the nonflat Pomeranchukon trajectory and using the eikonal model, have obtained good fits to the Serpukhov data for pp scattering. Theoretical difficulties arising in the calculations using the Regge-eikonal model have been recently discussed by Swift.[15] Koshaka and Takagi[16] have taken a flat Pomeranchukon whose residue is proportional to the square of a form factor of the proton. Although they have obtained good fits to the Serpukhov data, the fit is poor for the ISR (CERN Intersecting Storage Rings) data. Kawasaki and Yonezawa[17] have proposed a simple two-channel diffraction model which is consistent with the observed behavior of the forward slopes for pp scattering alone. Leader and Pennington[18] have introduced a new kinematic Lorentz-invariant variable which succeeds in explaining all the existing data for the slopes of pp and K^+p scattering which are exotic in the s channel. Pinsky[19] has proposed a set of kinematic variables which explains dips and breaks observed in pp and $\bar{p}p$ elastic diffraction scattering. A geometrical Regge model was proposed by Barger and Cline[20] to account for the shrinkage-antishrinkage pattern of elastic hadron-hadron scattering. It has been recently[21] pointed out that there is not even a qualitative explanation of the shrinkage-antishrinkage pattern. An empirical extrapolation rule $b = b_0 + b_1 s^{-1/2}$ proposed by Barger, Geer, and Phillips[22,23] successfully correlates the data for pp and $\bar{p}p$ slope parameters. This according to the authors may come from a Regge pole and cut model, a cancellation of parameters occurring for pp scattering. Carreras and White[24] have studied diffraction slopes for pp, $\bar{p}p$, K^+p, K^-p scattering by introducing a dipole form factor and an energy-dependent interaction term into the Chou-Yang model. Their result accounts only for the gross high-energy behavior of the slope parameter.

III. THE CONFORMAL MAPPING

Recently a model to describe the high-energy scattering of hadrons was proposed by the present authors[25] which incorporates the assumed analytic properties of scattering amplitudes. Here we show that using similar conformal mapping, the model can consistently explain the main features of all the existing data for forward slopes of pp, K^+p scattering at all measured energies and partially explain the intermediate- to high-energy behavior in case of the nonexotic processes $\bar{p}p$ and K^-p.

The main idea is to emphasize the need for maximal use of Mandelstam analyticity to propose theories of high-energy scattering. As has been already noted, the scattering near very forward angles is mainly due to the imaginary part of the amplitude and the imaginary part of the amplitude is an analytic function except for the location of the cuts given by the Mandelstam spectral functions. Since the spectral function boundary is curved, the location of the start of the cut changes with energy. We shall show that the variation of the slope parameter is related to the variation in the location of the start of this cut. So the shape of the boundary of the spectral function can be inferred by studying the dependence of the slope parameter on energy.

In Ref. 25 the elastic cuts of the scattering amplitude in the $x=\cos\theta$ plane were mapped on to the branches of a parabola with the origin as the focus in the z plane, and the entire cut x plane of analyticity was mapped into the interior of the parabola. The scattering amplitude was then expanded in Laguerre polynomials in the new mapped variable with a suitable weight factor.

To apply this idea to the slopes of elastic hadron-hadron collisions we consider the $x=\cos\theta$ plane in which the right-hand cut extends from $x=x_+(s)$ to ∞ and the left-hand cut extends from $x=-x_-(s)$ to $-\infty$, the physical region lying from $x=-1$ to $x=+1$. We fold the x plane in such a way that the left- and right-hand cuts coincide. The physical assumption involved in coinciding the start of the cuts is to weight equally the right- and left-hand cut contributions. One can fold to an arbitrary point for unequal-mass scattering, but this will introduce another parameter to the theory. The conformal mapping

$$y=2x+x_- - x_+ \tag{4}$$

places the cuts symmetrically with respect to the origin in the y plane. The points $x=+1$ and $x=x_+$ are mapped onto the points

$$y_{\max}=2+x_- - x_+ \tag{5}$$

and

$$y_{\text{in}}=x_- + x_+ , \tag{6}$$

respectively. We then apply the transformation

$$\omega=\frac{{y_{\max}}^2-y^2}{{y_{\text{in}}}^2-{y_{\max}}^2}, \tag{7}$$

which folds the cuts into the region $-\infty\leqslant\omega\leqslant-1$ of the negative real axis of the ω plane and the physical region is mapped into the region

$$0\leqslant\omega\leqslant\frac{{y_{\max}}^2}{{y_{\text{in}}}^2-{y_{\max}}^2}$$

of the real axis. Finally the transformation

$$z=\frac{1}{\pi^2}(\sinh^{-1}\sqrt{\omega})^2 \tag{8}$$

maps the entire cut x plane into the interior of a parabola in the z plane with the origin as focus, the cuts being mapped onto the branches of the parabola. The variable z is the same as one obtained by Cutkosky and Deo[5] for forward angles. The fact that a simple exponential-like equation (1) fits the data indicates that the rate of convergence is determined by $b(s)$. So $b(s)$ is directly related to the distance of the forward angle to the nearest cut. The problem, however, is one of correct extrapolation to near $t=0$ which will be achieved more efficiently by our mapping. For small t and for $b(s,t)$ it is enough to represent the scattering cross section as[25,26]

$$\frac{d\sigma}{dt}=Ae^{-\alpha z}. \tag{9}$$

The mapping has been constructed with an aim to hypothesize that α is not an energy-dependent parameter, because as energy increases, the physical region spreads over the real axis from 0 to ∞ whereas the distance of the cut from $t=0$ for all energies is just $-\pi^2$. It is easy to see that the considerations presented above do not hold true if $x_+>x_-$, i.e., the right-hand cut is farther away than the left-hand cut. The forward angles do not lie closest to the cut and in such a situation α may not be energy-independent. This may happen for $\bar{p}p$ or K^-p scattering at lower energies.

Our Eq. (9) is assumed to be an adequate representation of shape factors for small angles in an energy-dependent analysis and α is a constant. The variation of slope parameter with energy which we define is given for small t as

$$b(s,t)=\frac{d}{dt}\ln\left(\frac{d\sigma}{dt}\right). \tag{10}$$

IV. GENERALIZED FORMULA FOR SLOPE PARAMETERS

In this section we study the slope parameters separately for pp, $\bar{p}p$, K^+p, and K^-p scattering and show that a single generalized formula holds for all these four processes. The analyticity structures of scattering amplitudes for nucleon-nucleon scattering and kaon-nucleon scattering are shown in Fig. 1 and Fig. 2. Boundaries (a), (b), (e), and (f) in Figs. 1 and 2 represent only the over-all boundaries and we have neglected the detailed overlapping structures which arise in kaon-nucleon scattering. For pp elastic scattering the Mandelstam variables are

$$\begin{aligned} s&=4(q^2+m^2),\\ t&=-2q^2(1-\cos\theta),\\ u&=-2q^2(1+\cos\theta), \end{aligned} \tag{11}$$

where θ is the c.m. scattering angle and q is the magnitude of the momentum in the c.m. system, and m is the mass of the proton. It is well known that the boundary of the spectral function ρ_{st} is given by hyperbolas [curve (a), Fig. 1], asymptotes to the extreme hyperbolas being $t_c=4m_\pi{}^2$, $s_{\text{th}}=4m^2$. At sufficiently lower energies the con-

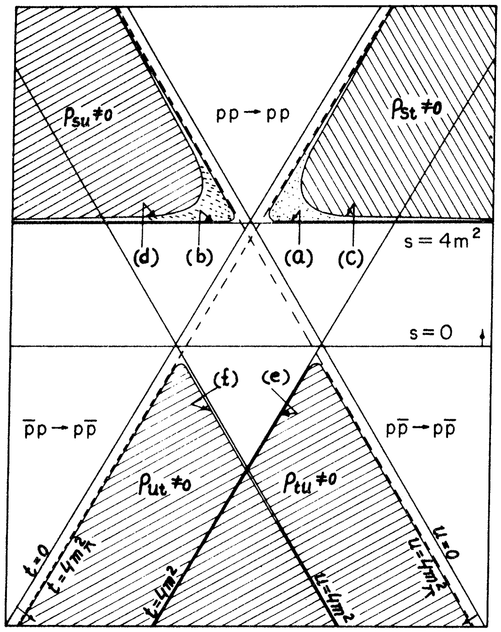

FIG. 1. Analytic properties of the Mandelstam amplitudes for nucleon-nucleon scattering. Curves (a), (b), (e), and (f) indicate theoretical predictions for $\lambda = 0.139$ GeV. Curves (c) and (d) indicate the new boundaries of ρ_{st} and ρ_{su} predicted from this analysis with $\lambda = 0.579$ GeV.

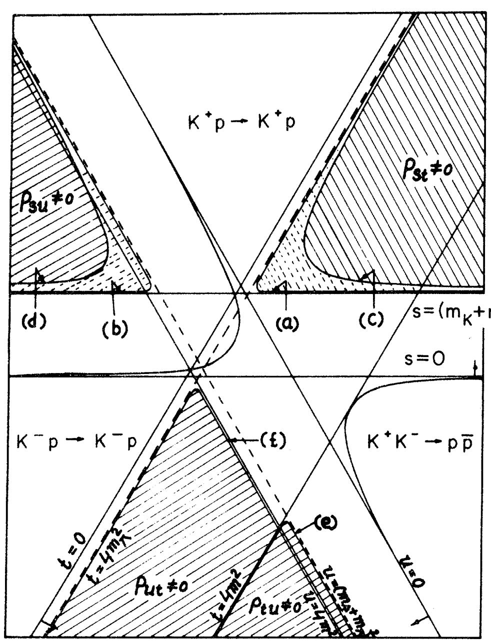

FIG. 2. Analytic properties of the Mandelstam amplitudes for kaon-nucleon scattering. Curves (a), (b), (e), and (f) indicate over-all theoretical predictions for $\lambda = 0.139$ GeV. Curve (c) indicates the new boundary for ρ_{st} with $\lambda_1 = 0.579$ GeV, and curve (d) indicates the new boundary for ρ_{su} with $\lambda_2 = 0.597$ GeV predicted from this analysis.

tribution of the second term in Eq. (2) becomes important in deciding the position of the elastic cut. However, keeping the asymptotes unchanged one can still represent the hyperbola by the formula

$$t_{R\,pp} = 4m_\pi^{\,2} + \frac{4\lambda^4}{s-4m^2}, \tag{12}$$

where $t_{R\,pp}$ stands for the right-hand elastic cut position for pp scattering in the t plane. The curvature of the portion of the hyperbola around its turning point is now significantly affected by λ. Similarly the boundary of the spectral function ρ_{su} can be represented by

$$t_{L\,pp} = 4m_\pi^{\,2} + \frac{4\lambda^4}{s-4m^2}. \tag{13}$$

We write

$$x_+ = 1 + t_{R\,pp}/2q^2,$$
$$x_- = 1 + t_{L\,pp}/2q^2. \tag{14}$$

Now using Eqs. (4)–(14) we observe that for pp scattering

$$b_{pp}(s,t) = \frac{\alpha_{pp}}{t_{R\,pp}}\left(1 - \frac{t_{R\,pp}-2t}{4q^2+t_{L\,pp}}\right) \times \frac{\ln\{\sqrt{\omega}+[(\omega+1)]^{1/2}\}}{[\omega(\omega+1)]^{1/2}}. \tag{15}$$

Equation (15) expresses a t dependence of the slope parameter in addition to its s dependence. Experimental data[9-13] also indicate that b has a t dependence at fixed s. The exact t dependence of $b(s,t)$ from Eq. (9) may be misleading, however. For $\bar{p}p$ scattering we observe that

$$t_{L\,\bar{p}p} = 4m^2 + \frac{4\lambda^4}{s-4m_\pi^{\,2}} \tag{16}$$

which represents the boundary of ρ_{su}. The boundaries of ρ_{tu} and ρ_{ut} are represented by two hyperbolas [curves (e) and (f), Fig. 1]. Thus $t_{R\,\bar{p}p}$ will be represented by the minimum of t_1 and t_2 as specified below:

$$t_1 = 4m_\pi^{\,2} + \frac{4\lambda_1^{\,4}}{s-4m^2},$$
$$t_2 = 4m^2 + \frac{4\lambda_1^{\,4}}{s-4m_\pi^{\,2}}, \tag{17}$$

where $\lambda_1 = m_\pi$ for the boundaries. In formulas (16) and (17) s refers to the square of the c.m. energy of the $\bar{p}p$ system. Proceeding in the same way as for pp scattering we see that

$$b_{\bar{p}p}(s,t)=\frac{\alpha_{\bar{p}p}}{t_{R\bar{p}p}}\left(1-\frac{t_{R\bar{p}p}-2t}{4q^2+t_{L\bar{p}p}}\right)\times\frac{\ln\{\sqrt{\omega}+[(\omega+1)]^{1/2}\}}{[\omega(\omega+1)]^{1/2}}. \quad (18)$$

For K^+p elastic scattering

$$t_{RK^+p}=4m_\pi{}^2+\frac{4\lambda_1{}^4}{s-(m_K+m)^2} \quad (19)$$

and

$$t_{LK^+p}=(m_\Lambda+m_\pi)^2+\frac{4\lambda_2{}^4}{s-(m_K+m)^2}, \quad (20)$$

where m_K is the mass of the kaon and m_Λ is the mass of the Λ hyperon. Thus we find in a similar manner

$$b_{K^+p}(s,t)=\frac{\alpha_{K^+p}}{t_{RK^+p}}\left(1-\frac{t_{RK^+p}-2t}{4q^2+t_{LK^+p}-\Delta/s}\right)\times\frac{\ln\{\sqrt{\omega}+[(\omega+1)]^{1/2}\}}{[\omega(\omega+1)]^{1/2}}, \quad (21)$$

and $\Delta=(m^2-m_K{}^2)^2$. For K^-p elastic scattering

$$t_{LK^-p}=(m_\Lambda+m_\pi)^2+\frac{4\lambda_2{}^4}{s-(m_K+m)^2}, \quad (22)$$

and t_{RK^-p} is given by the minimum between t_1 and t_2 as specified by the following formula [curves (e) and (f) in Fig. 2]:

$$t_1=4m^2+\frac{4\lambda_3{}^4}{s-(m_\Lambda+m_\pi)^2}, \quad (23)$$

$$t_2=4m_\pi{}^2+\frac{4\lambda_4{}^4}{s-(m_K+m)^2}. \quad (24)$$

Thus

$$b_{K^-p}(s,t)=\frac{\alpha_{K^-p}}{t_{RK^-p}}\left(1-\frac{t_{RK^-p}-2t}{4q^2+t_{LK^-p}-\Delta/s}\right)\times\frac{\ln\{\sqrt{\omega}+[(\omega+1)]^{1/2}\}}{[\omega(\omega+1)]^{1/2}}. \quad (25)$$

In formulas (22)–(25) s, q^2, and t refer to the K^-p system.

It is interesting to note that for the above four processes the slope parameters are reproduced by a general formula

$$b(s,t)=\frac{\alpha}{t_R}\left(1-\frac{t_R-2t}{4q^2+t_L-\Delta/s}\right)\times\frac{\ln\{\sqrt{\omega}+[(\omega+1)]^{1/2}\}}{[\omega(\omega+1)]^{1/2}}, \quad (26)$$

where $\Delta=0$, for equal-mass elastic scattering. When $t=0$, Eq. (26) gives

$$b(s,0)=\frac{\alpha}{t_R}\left(1-\frac{t_R}{4q^2+t_L}\right). \quad (27)$$

Formula (27) can be compared with the result of Leader and Pennington[18] (for the process $m+M\to m+M$)

$$b(s,0)=\beta_0\left[1-\frac{2(M^2+m^2)}{s}+\frac{(M^2-m^2)^2}{s^2}\right]. \quad (28)$$

We observe from Eq. (26) that $b(s,t)$ decreases with an increase in the magnitude of momentum transfer $|t|$. The decrease of the slope parameter for increasing values of $|t|$ has been explained in Ref. 23 by considering a curved P trajectory, a curved P residue, and P with destructive cuts and also in Ref. 27 by considering current-current interaction in the droplet model. The experimental information concerning such types of behavior has been reviewed by Carrigan.[28]

It should be noted[29] that the expression for $y_{\max}$ [Eq. (5)] is true only when $4q^2+t_L\geq t_R$. This formula is different when $t_R>t_L$, a condition which is satisfied when $q^2\to 0$ in K^-p elastic scattering and can be easily verified from Fig. 2.

V. DETERMINATION OF EFFECTIVE BOUNDARIES OF SPECTRAL FUNCTIONS

In this section we show how experimental data are used to predict the boundaries of spectral functions according to our new formula for slope parameters.

(a) pp scattering. We tried to parametrize pp scattering data[9-13] by varying λ, thereby changing the shape of the boundary of spectral functions in the low-energy region. For $\lambda=0.139$ GeV, which gives the theoretical boundaries of ρ_{st} and ρ_{su} [curves (a) and (b) of Fig. 1] we find a sharp rise of the slope parameter after threshold and after s reaches a few GeV^2 the slope parameter becomes a constant. This is shown by curve I in Fig. 3 and gives only the gross behavior of the slope parameter at high energy. The variation of the slope parameter at lower, intermediate, and high energies is correctly explained by taking λ nearly equal to 4 times the pion mass. Thus Eq. (15) gives a good fit by eye to the Serpukhov data, ISR (CERN Intersecting Storage Rings) data, and data at low energies for

$$|t|=0.05\text{ GeV}^2,\quad \alpha_{pp}=1.28,\quad \text{and}\quad \lambda=0.579\text{ GeV}. \quad (29)$$

This fit has been shown by curve II in Fig. 3. In Fig. 3 we have also shown the variation of slope parameters with $|t|$ while the other parameters remain the same as in curve II.

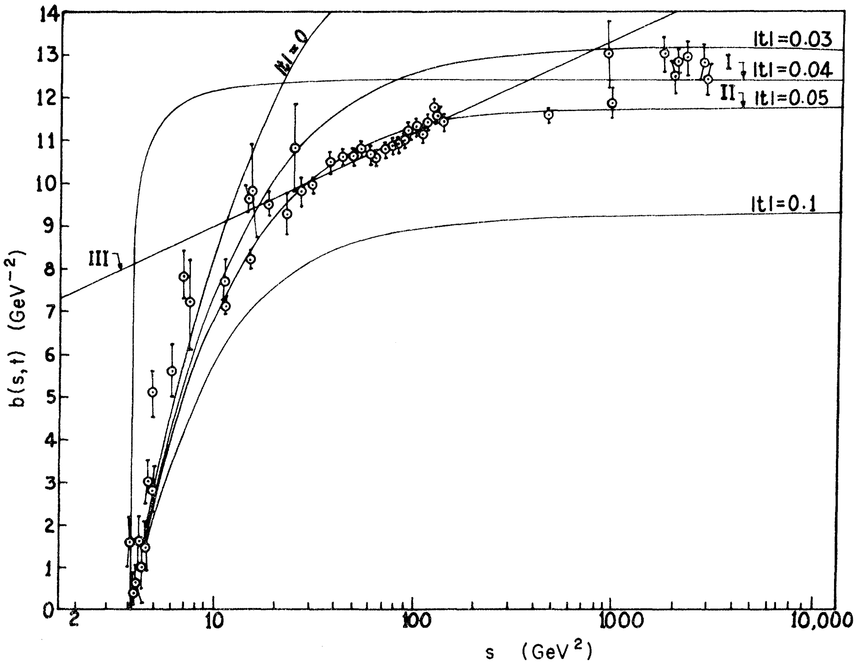

FIG. 3. The slope parameter of the forward peaks for pp elastic scattering as a function of s and for different values of t (t is in units of GeV^2). Only those data points for which $|t| \leq 0.17$ GeV^2 have been taken from Refs. 9–13. The solid lines are our predictions. Curve I is the prediction of the theoretical boundaries. Curve II is the curve obtained with the parameters given in (29). The straight-line curve III is based on a fit to the Serpukhov data[10]: $b(s,0) = 6.8 + 0.94 \ln s$.

(b) $\bar{p}p$ scattering. For $\bar{p}p$ scattering the experimental data[9] on slope parameters fluctuate rapidly with energy in the low-energy region due to resonances. We tried to fit the data with Eq. (18) by keeping the value of λ fixed at 0.579 GeV (the value predicted by fits to the pp slope parameters) and varying λ_1. We find that a reasonably good interpolation for the $\bar{p}p$ slope parameters is obtained for

$$|t| = 0.05 \text{ GeV}^2,$$

$$\alpha_{\bar{p}p} = 1.467, \tag{30}$$

and

$$\lambda_1 = 0.139 \text{ GeV}.$$

We find that above a few GeV/c of incident laboratory momentum our slope approaches its constant asymptotic value. This is shown by curve I in Fig. 4. We find that the value of λ_1 corresponds to the pion mass which is the theoretical value. In Fig. 4 we have also shown the variation of slope parameter with $|t|$.

With the knowledge of λ and λ_1 we can now plot the effective shape of the spectral functions. This has been shown in Fig. 1. Curves (c) and (d) represent effective boundaries of ρ_{st} and ρ_{su} corresponding to the value of $\lambda = 0.579$ GeV, and $\lambda_1 = 0.139$ GeV gives the theoretical boundaries [curves (e) and (f) in Fig. 1]. Curves (a) and (b) in Fig. 1 correspond to the theoretical boundaries of ρ_{st} and ρ_{su}, respectively, for $\lambda = 0.139$ GeV. It is well known that at least at low energies the two-pion cut is very weak and our analysis corroborates this view.

(c) K^+p scattering. For K^+p scattering the process of parametrization is the same as for pp scattering. A reasonably good fit to the experimental data is obtained by Eqs. (19), (20), and (21) for

$$|t| = 0.05 \text{ GeV}^2,$$

$$\alpha_{K^+p} = 0.852,$$

$$\lambda_1 = 0.578 \text{ GeV}, \tag{31}$$

and

$$\lambda_2 = 0.597 \text{ GeV}.$$

This fit is shown by curve II in Fig. 5. Curve I of Fig. 5 shows the theoretical predictions for $\lambda_1 = \lambda_2 = 0.139$ GeV and gives only the gross features of very-high-energy scattering.

(d) K^-p scattering. The experimental data for K^-p elastic scattering also show rapid fluctuations in the low-energy region due to the presence of resonances. While trying to fit the data with Eq. (25) we kept the value of λ_2 fixed at 0.597 GeV as

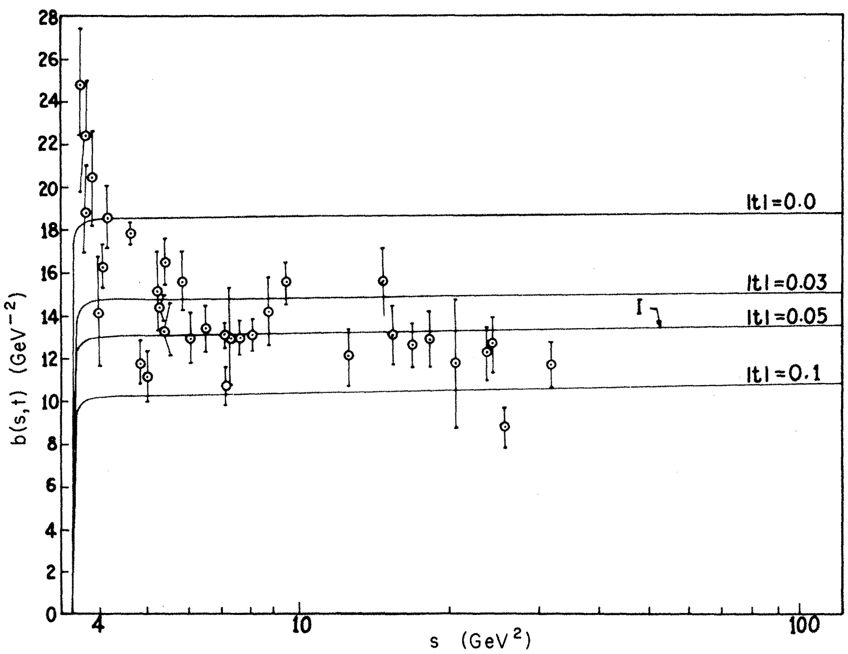

FIG. 4. Slope parameter of the forward peaks for $\bar{p}p$ elastic scattering as a function of s and for different values of t (in units of GeV^2). Curve I is obtained with the parameters given in (30). The data points are from Ref. 9.

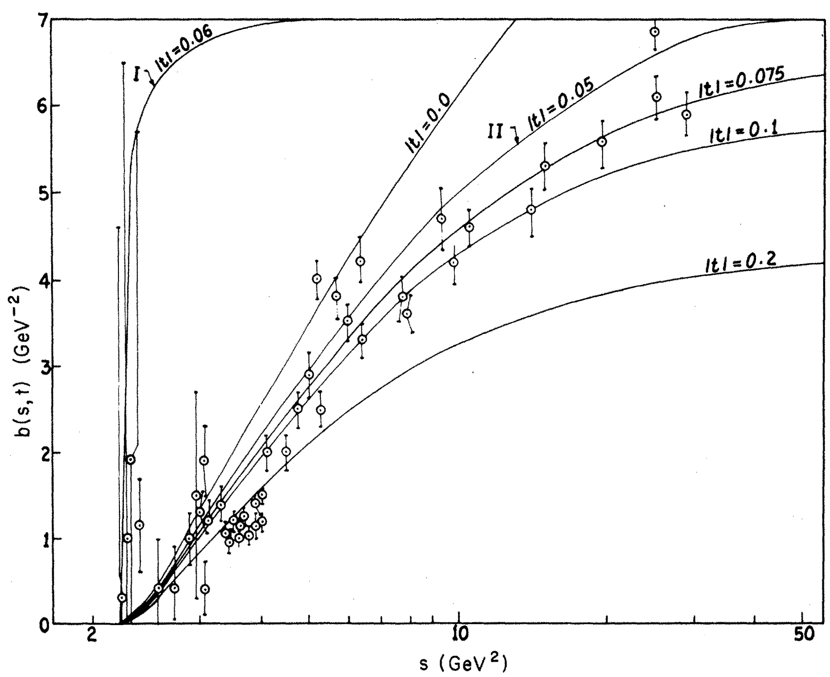

FIG. 5. Slope parameters of the forward peaks for K^+p elastic scattering as a function of s and for different values of t (t in units of GeV^2). The data points are from Ref. 9 and the solid lines are our predictions. Curve II is obtained from the parameters given in (31). Curve I is the prediction of the theoretical boundaries (a) and (b) of Fig. 2 for $\lambda_1 = \lambda_2 = 0.139$ GeV.

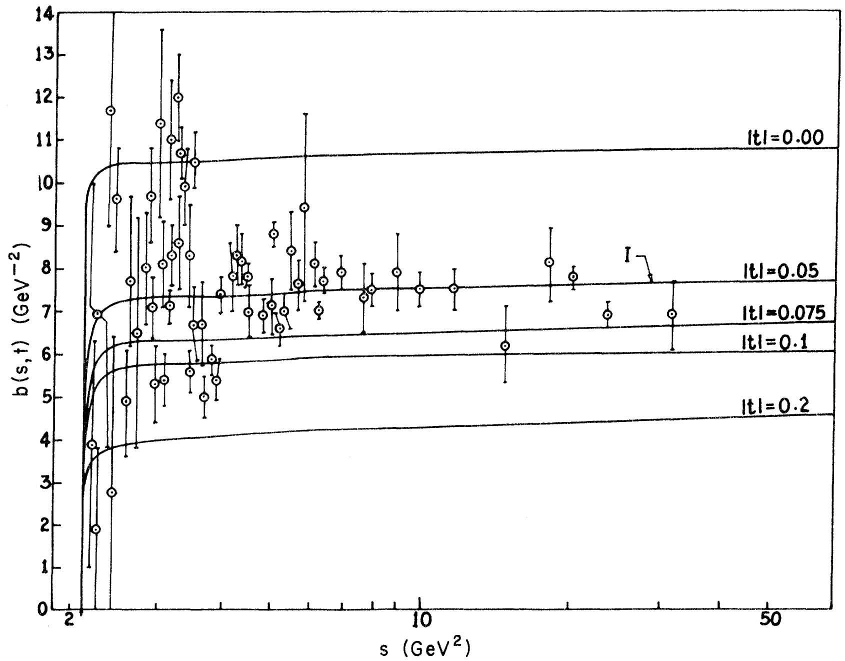

FIG. 6. Slope parameters for the forward peaks as a function of s and for different values of t (in units of GeV^2) for K^-p elastic scattering. The data points are from Ref. 9. The solid lines are our predictions. Curve I is the prediction with the parameters given in (32).

predicted by the fits to the K^+p data and found reasonably good fits for

$$|t| = 0.05 \text{ GeV}^2,$$

$$\alpha_{K^-p} = 0.840,$$

and (32)

$$\lambda_3 = \lambda_4 = 0.139 \text{ GeV}.$$

This has been shown by curve I in Fig. 6. In Fig. 6 we have also shown the variation of the slope parameters with $|t|$. We find from curve I that the slope parameter approaches its asymptotic limit after a few GeV/c of laboratory momentum. The values of λ_3 and λ_4 now correspond to the pion mass, which is again the theoretical prediction.

With the knowledge of λ_1, λ_2, λ_3, and λ_4, we can now plot the effective boundaries ρ_{st}, ρ_{su}, ρ_{tu}, and ρ_{ut}. Curves (a) and (b) in Fig. 2 are the theoretical boundaries corresponding to the values of λ_1 and λ_2, each equal to 0.139 GeV. Curves (c) and (d) correspond to $\lambda_1 = 0.578$ GeV and $\lambda_2 = 0.597$ GeV, respectively. Curves (e) and (f) are the theoretical boundaries which correspond to the values of λ_3 and λ_4, each equal to the pion mass. This again confirms our earlier observation that at low energies the strength of the discontinuity across the two-pion cut is weak.

VI. CONCLUSION

To summarize we observe that our parabolic variable gives a good account of the slope parameters of the forward peaks for pp, $\bar{p}p$, K^+p, and K^-p elastic scattering at all measured energies. The shapes of the boundaries of the spectral functions ρ_{st} and ρ_{su} near their turning points play an important role in determining the shrinkage in pure diffraction scattering. For very high energies, the constancy of the slope parameters can be visualized as being given by the asymptotes to the boundaries of the spectral functions.

As has been pointed out earlier, a new feature appears in K^-p scattering as $q^2 \to 0$. In this limit t_{RK^-p} becomes greater than t_{LK^-p} and the expression for $y_{\max}$ becomes different.[29] The calculated value of the slope parameter becomes slightly negative at $q^2 = 0$. There is a possibility that this phenomenon can also arise in $\bar{p}p$ scattering for suitable effective boundaries ρ_{tu} and ρ_{ut} of Fig. 1. It is the feeling of the present authors that this peculiar feature may be incorporated into some conformal mapping to explain the observed shrinkage and antishrinkage pattern in $\bar{p}p$ and K^-p scattering.[21]

Recently from considerations of analyticity and threshold requirements in the t channel, the structure in cross sections observed near the crossing point $|t| \sim 4\, m_\pi^2$ has been explained by Barshay and Chao.[30] Our formula has been shown to be highly sensitive to the variation with $|t|$ and we hope it can adequately account for the structures observed in various hadron-hadron collision processes.

---

[1] C. B. Chiu, Rev. Mod. Phys. 41, 640 (1969).

[2] J. G. Taylor, M. J. Moravcsik, and J. L. Uretsky, Phys. Rev. 113, 689 (1959); P. Cziffra and M. J. Moravcsik, *ibid.* 116, 226 (1959). These authors have evaluated pion-nucleon coupling by some conjecture concerning the analyticity of photoproduction and the n-p scattering amplitude and by using experimental data on the differential cross sections.

[3] G. F. Chew and F. E. Low, Phys. Rev. 101, 1570 (1956).

[4] R. E. Cutkosky and B. B. Deo, Phys. Rev. Letters 20, 1272 (1968).

[5] R. E. Cutkosky and B. B. Deo, Phys. Rev. 174, 1859 (1968).

[6] S. Ciulli, Nuovo Cimento 61A, 787 (1969).

[7] Y. A. Chao, Phys. Rev. Letters 25, 309 (1970).

[8] R. E. Cutkosky, Ann. Phys. (N.Y.) 54, 350 (1969).

[9] T. Lasinski, R. Levi Setti, B. Schwarzschild, and P. Ukleja, Nucl. Phys. B37, 1 (1972).

[10] G. G. Beznogikh, A. Buyak, K. I. Iovchen, L. F. Kirillova, P. K. Markov, B. A. Morozov, V. A. Nikitin, P. V. Nomokonov, M. G. Shafranova, V. A. Sviriodov Truong Bien, V. I. Zayachki, N. K. Zhidkov, L. S. Zolin, S. B. Nurushev, and V. L. Solovianov, Phys. Letters 30B, 274 (1969).

[11] M. Holder, E. Radermacher, A. Staude, G. Barbiellini, P. Darriulat, M. Hansroul, S. Orito, P. Palazzi, A. Santroni, P. Strolin, K. Tittle, J. Pilcher, C. Rubbia, G. De Zorzi, M. Macri, G. Sette, C. Grosso-Pilcher, A. Fainberg, and G. Maderni, Phys. Letters 35B, 355 (1971).

[12] U. Amaldi, R. Biancastelli, C. Bosio, G. Matthiae, J. V. Allaby, W. Bartel, G. Cocconi, A. N. Diddens, R. W. Dobinson, V. Elings, J. Litt, L. S. Rochester, and A. M. Wetherell, Phys. Letters 36B, 504 (1971).

[13] G. Barbiellini, M. Bozzo, P. Darriulat, G. Diambrini Palazzi, G. De Zorzi, A. Fainberg, M. I. Ferrero, M. Holder, A. McFarland, G. Maderni, S. Orito, J. Pilcher, C. Rubbia, A. Santroni, G. Sette, A. Staude, P. Strolin, and K. Tittel, Phys. Letters 39B, 663 (1972).

[14] J. M. Kaplan and D. Schiff, Lett. Nuovo Cimento 3, 19 (1970).

[15] Arthur R. Swift, Phys. Rev. D 5, 1400 (1972).

[16] Y. Kohsaka and F. Takagi, Lett. Nuovo Cimento 4, 747 (1970).

[17] M. Kawasaki and M. Yonezawa, Progr. Theoret. Phys. (Kyoto) 46, 1295 (1971); M. Kawasaki, M. Kobayashi, and M. Yonezawa, *ibid.* 44, 557 (1970); Lett. Nuovo Cimento 3, 655 (1970).

[18] E. Leader and M. R. Pennington, Phys. Rev. Letters 27, 1325 (1971).

[19] Stephen S. Pinsky, Phys. Rev. Letters 27, 1548 (1971).

[20] V. Barger and D. Cline, Nucl. Phys. B23, 227 (1970).

[21] T. J. Weare, Nuovo Cimento 9A, 173 (1972).

[22] V. Barger, K. Geer, and R. J. N. Phillips, Phys. Letters 36B, 343 (1971).

[23] V. Barger, K. Geer, and R. J. N. Phillips, Phys. Letters 36B, 350 (1971).

[24] B. Carreras and J. N. J. White, Nucl. Phys. B42, 95 (1972).

[25] B. B. Deo and M. K. Parida, Phys. Rev. Letters 26, 1609 (1971).

[26] R. E. Cutkosky, Nucl. Phys. B13, 351 (1969).

[27] S. Y. Lo and G. D. Thomson, Lett. Nuovo Cimento 3, 223 (1972).

[28] R. A. Carrigan, Jr., Phys. Rev. Letters 24, 168 (1970).

[29] We observe from Fig. 2 and and formulas (22), (23), and (24) for K^-p scattering that very near the threshold value of s we have $t_{LK^-p} > t_{RK^-p}$ for which

$$y_{\max}{}^2 = [2 - (x_- - x_+)]^2,$$

and this yields $b_{K^-p}|_{q^2=0} = -0.04$. This has been indicated by an arrow crossing the s axis in Fig. 6.

[30] S. Barshay and Y. A. Chao, Phys. Rev. Letters 29, 753 (1972).